

# Ambipolar Tetrafluorodiphenylethene-Based Donor–Acceptor Copolymers: Synthesis, Properties, Backbone Conformation and Fluorine-Induced Conformational Locks

Weifeng Zhang,<sup>†,§</sup> Zupan Mao,<sup>†,§</sup> Zhihui Chen,<sup>†</sup> Jianyao Huang,<sup>†</sup> Congyuan Wei,<sup>†</sup>  
Dong Gao,<sup>†</sup> Zuzhang Lin,<sup>‡</sup> Hao Li,<sup>‡</sup> Liping Wang,<sup>\*,‡</sup> and Gui Yu<sup>\*,‡,#</sup>

<sup>†</sup>*Beijing National Laboratory for Molecular Sciences, Institute of Chemistry, Chinese Academy of Sciences, Beijing 100190, P. R. China. E-mail: yugui@iccas.ac.cn*

<sup>‡</sup>*School of Material Science and Engineering, University of Science and Technology Beijing, Beijing 100083, P. R. China. E-mail: lpwang@mater.ustb.edu.cn*

## 1. Thermogravimetric analysis (TGA) of TFPE-based copolymers.

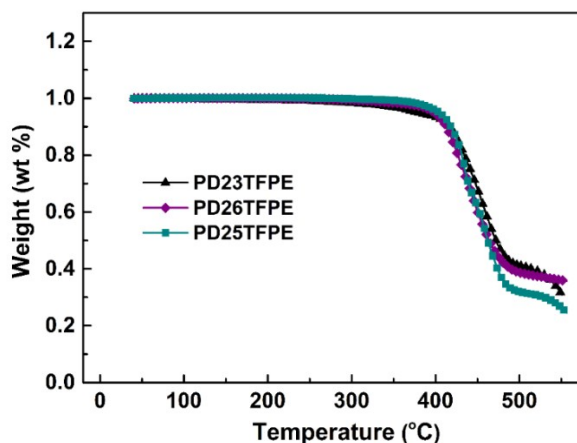


**Figure S1.** TGA traces of TFPE-based copolymers.

2. Differential scanning calorimetry (DSC) of TFPE-based copolymers.

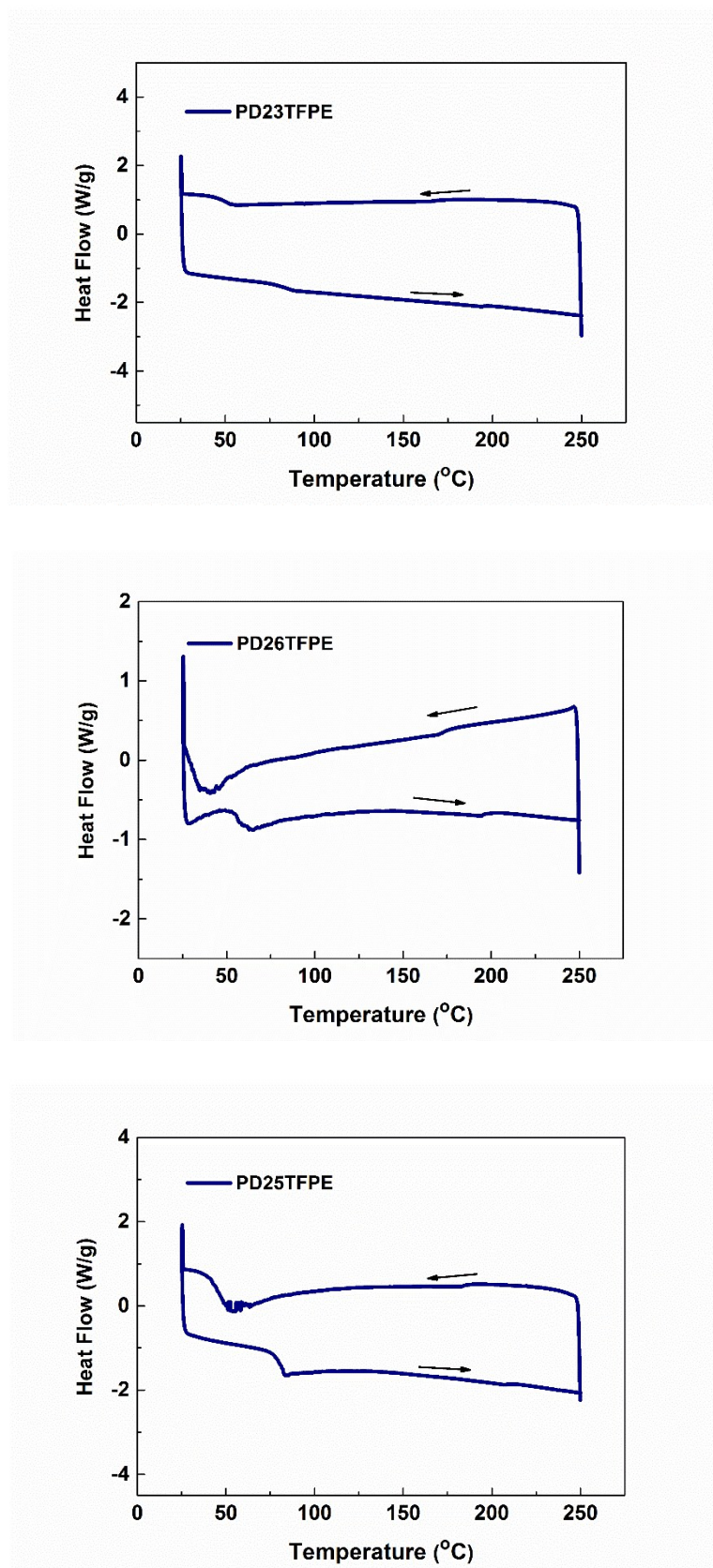
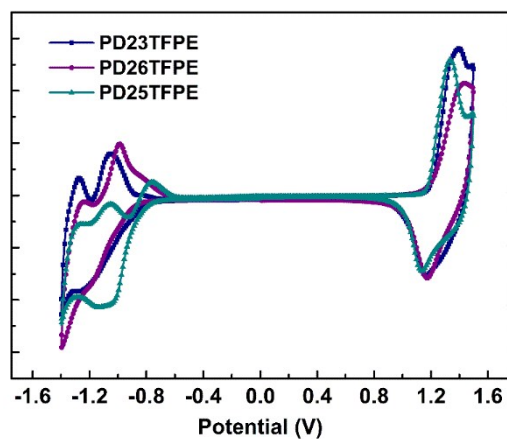


Figure S2. DSC curves of TFPE-based copolymers.

3. Electrochemical properties of TFPE-based copolymers.



**Figure S3.** CV traces of TFPE-based copolymers.

4. Optimized molecular structure and dihedral angle of the TFPE-based copolymers.

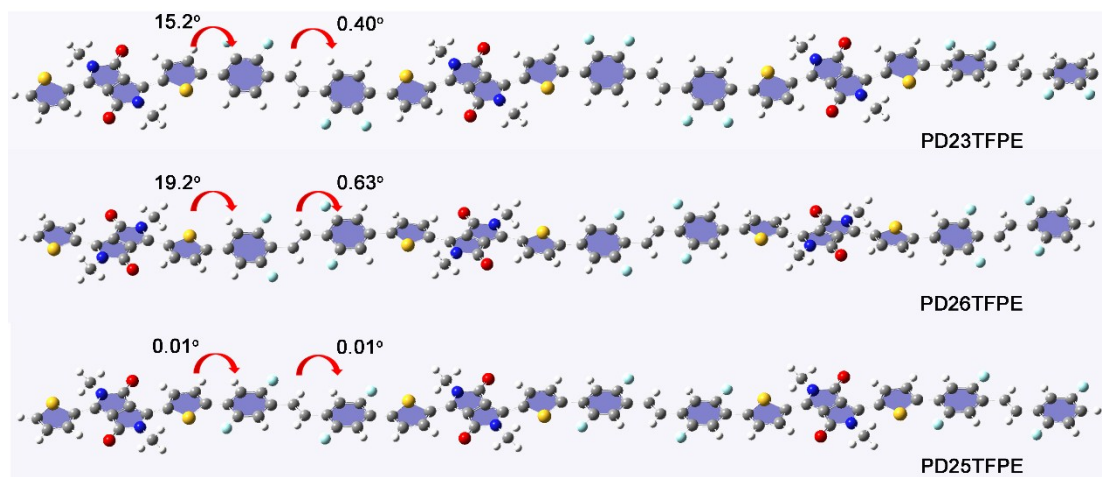


**Figure S4.** Optimized molecular structure and dihedral angle of the TFPE-based copolymers (trimer) (B3LYP/6-31G\*).

5. Annealing temperature-dependent device performance of TFPE-based copolymers.

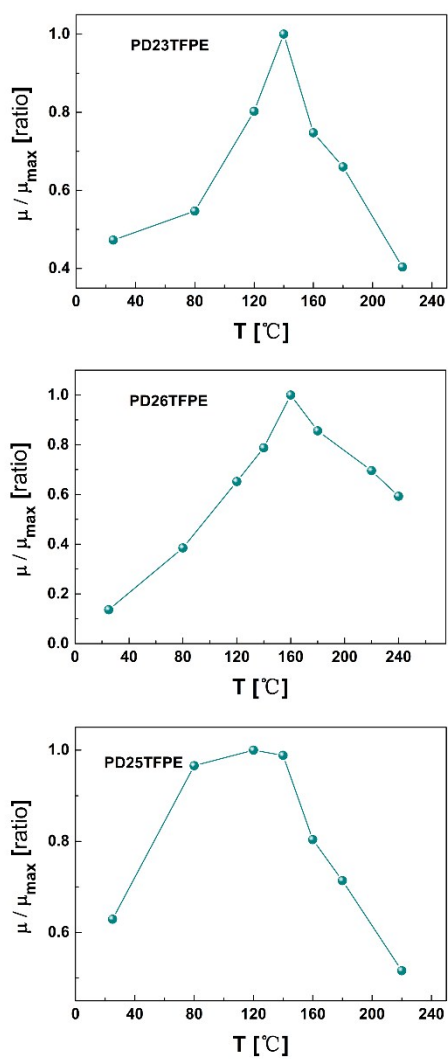


**Figure S5.** Annealing temperature-dependent mobilities of PD23TFPE, PD26TFPE, and PD25TFPE.

6. The BGBC FET device performance of TFPE-based copolymer.

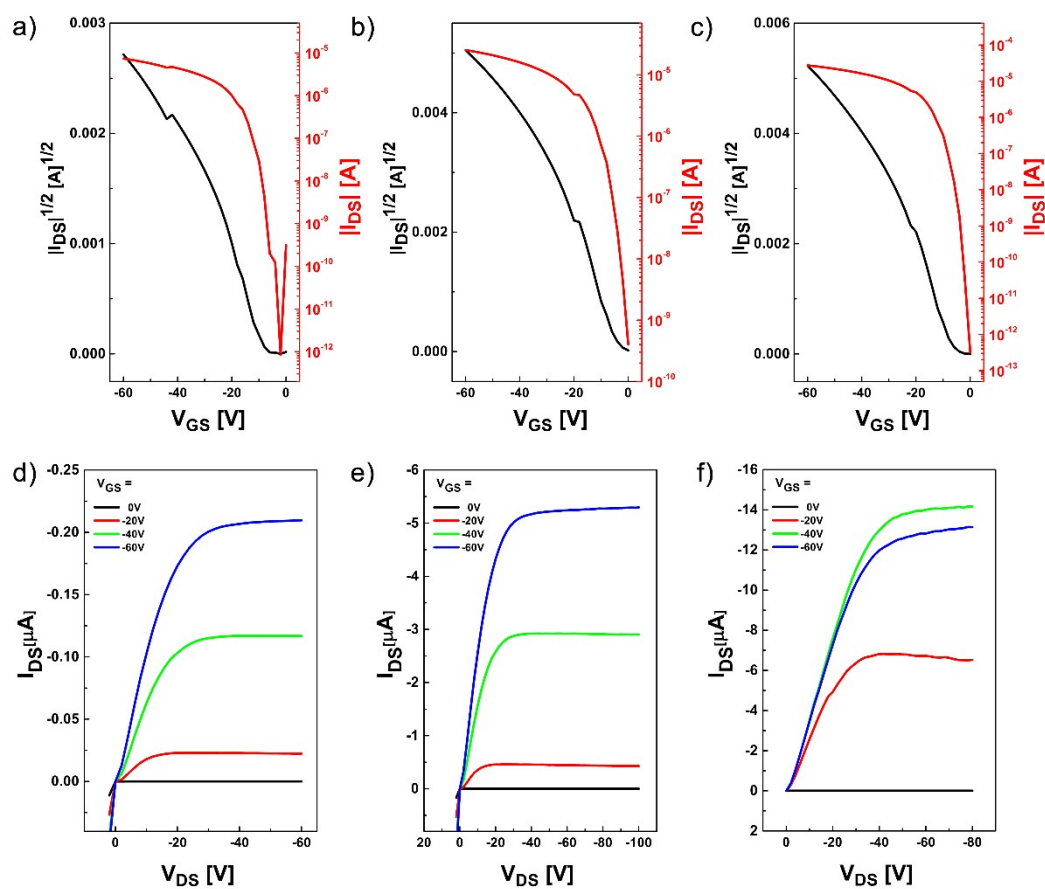


**Figure S6.** Typical transfer and output characteristics of TFPE-based copolymers in BGBC devices. (a,c) PD23TFPE, (b,e) PD26TFPE, and (c,f) PD25TFPE.

7. AFM images of the TFPE-based copolymers as-spun films.

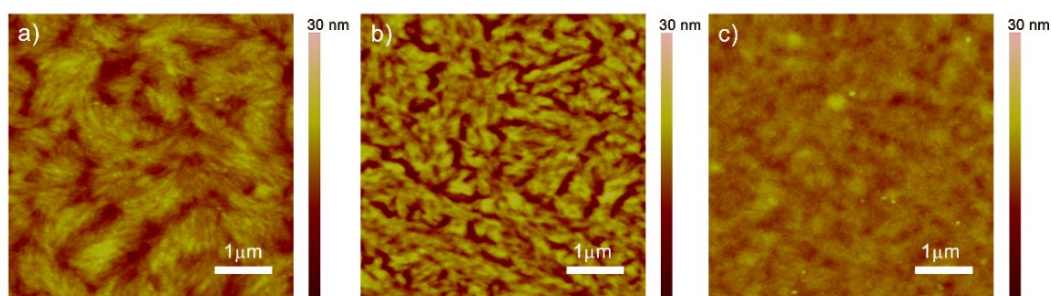


**Figure S7.** AFM topography images of the TFPE-based copolymers as-spun films on OTS-modified  $SiO_2/Si$  substrates. a) PD23TFPE, b) PD26TFPE, and c) PD25TFPE.

## 8. GIXRD images of the TFPE-based copolymers as-spun films.

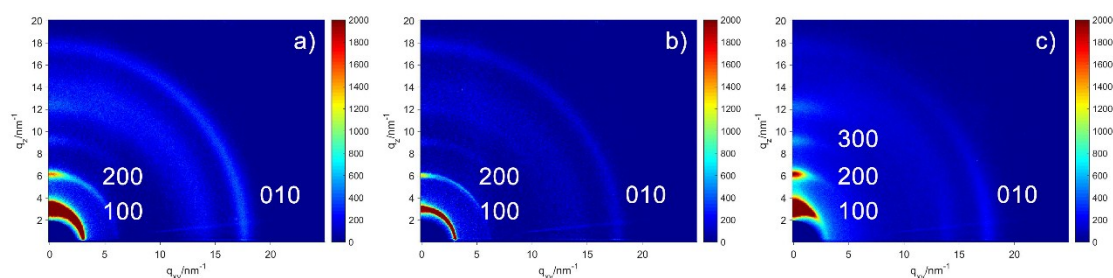


**Figure S8.** 2D-GIXRD patterns of the TFPE-based copolymers as-spun films on OTS-modified SiO<sub>2</sub>/Si substrates. a) PD23TFPE, b) PD26TFPE, and c) PD25TFPE.

## 9. X-ray crystallographic data

**Table S1.** Crystal data and structure refinement for 23TFPE, **6a**.

Identification code	sa4965-a
Empirical formula	C <sub>33</sub> H <sub>18</sub> F <sub>6</sub> S <sub>3</sub>
Formula weight	624.65
Temperature	173 K
Wavelength	0.71073 Å
Crystal system	Monoclinic
Space group	P 1 21/n 1
Unit cell dimensions	a = 6.538(3) Å    α = 90° b = 22.320(9) Å    β = 95.624(5)° c = 17.876(7) Å    γ = 90°
Volume	2596.0(18) Å <sup>3</sup>
Z	4
Density (calculated)	1.598 mg/m <sup>3</sup>
Absorption coefficient	0.354 mm <sup>-1</sup>
F(000)	1272
Crystal size	0.48 × 0.17 × 0.15 mm <sup>3</sup>
Theta range for data collection	0.912 to 25.200°
Index ranges	-7 ≤ h ≤ 7, -26 ≤ k ≤ 26, -20 ≤ l ≤ 21
Reflections collected	14426
Independent reflections	4653 [R(int) = 0.0558]
Completeness to theta = 26.000°	99.8 %
Absorption correction	Semi-empirical from equivalents
Max. and min. transmission	1.0000 and 0.786

Refinement method	Full-matrix least-squares on F <sup>2</sup>
Data / restraints / parameters	4653 / 81 / 389
Goodness-of-fit on F <sup>2</sup>	1.173
Final R indices [I>2σ(I)]	R1 = 0.1478, wR2 = 0.3519
R indices (all data)	R1 = 0.1579, wR2 = 0.3586
Extinction coefficient	n/a
Largest diff. peak and hole	1.482 and -0.638 e.Å <sup>-3</sup>

**Table S2.** Crystal data and structure refinement for 26TFPE, **2b**.

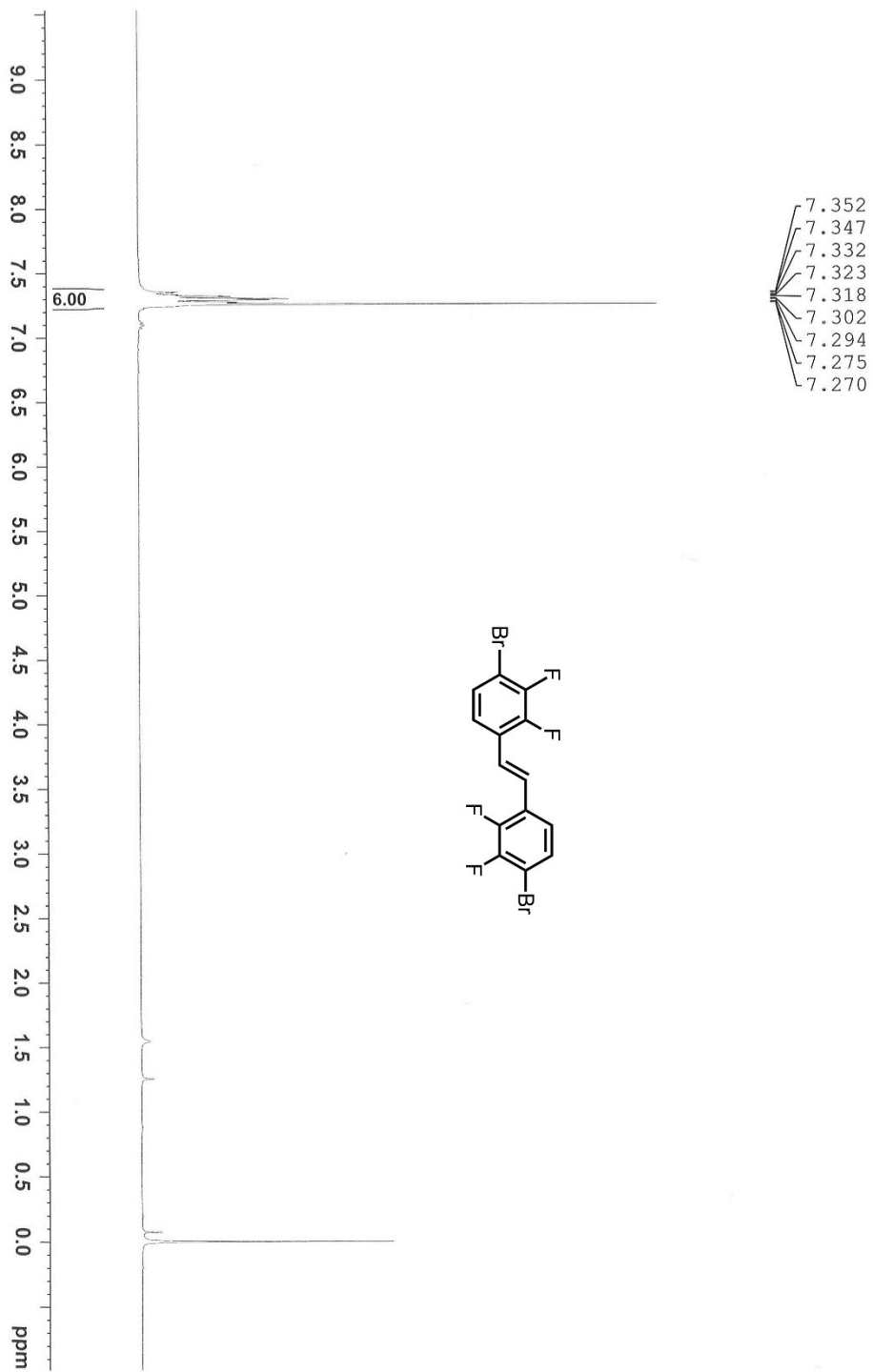
Identification code	sa3515
Empirical formula	C <sub>14</sub> H <sub>6</sub> Br <sub>2</sub> F <sub>4</sub>
Formula weight	410.01
Temperature	173.1500 K
Wavelength	0.71073 Å
Crystal system	Monoclinic
Space group	P 1 21/c 1
Unit cell dimensions	a = 10.453(4) Å    α = 90° b = 4.7776(16) Å    β = 91.545(6)° c = 12.787(5) Å    γ = 90°
Volume	638.4(4) Å <sup>3</sup>
Z	2
Density (calculated)	2.133 mg/m <sup>3</sup>
Absorption coefficient	6.382 mm <sup>-1</sup>
F(000)	392
Crystal size	0.47 × 0.38 × 0.07 mm <sup>3</sup>
Theta range for data collection	3.187 to 27.518°
Index ranges	-13 ≤ h ≤ 13, -6 ≤ k ≤ 6, -16 ≤ l ≤ 16
Reflections collected	5202
Independent reflections	1468 [R(int) = 0.0392]
Completeness to theta = 26.000°	99.8 %
Absorption correction	Semi-empirical from equivalents
Max. and min. transmission	1.0000 and 0.1259
Refinement method	Full-matrix least-squares on F <sup>2</sup>
Data / restraints / parameters	1468 / 0 / 91
Goodness-of-fit on F <sup>2</sup>	1.147
Final R indices [I>2σ(I)]	R1 = 0.0308, wR2 = 0.0721
R indices (all data)	R1 = 0.0332, wR2 = 0.0733

Extinction coefficient	n/a
Largest diff. peak and hole	0.401 and $-0.516 \text{ e.}\text{\AA}^{-3}$

**Table S3.** Crystal data and structure refinement for 25TFPE-T, **6c**.

Identification code	Sa4960b
Empirical formula	$\text{C}_{22}\text{H}_{12}\text{F}_4\text{S}_2$
Formula weight	416.44
Temperature	173.1500 K
Wavelength	0.71073 $\text{\AA}$
Crystal system	C 1 2 1
Space group	P 1 21/c 1
Unit cell dimensions	$a = 18.983(7) \text{ \AA}$ $\alpha = 90^\circ$ $b = 6.635(2) \text{ \AA}$ $\beta = 101.140(4)^\circ$ $c = 28.718(11) \text{ \AA}$ $\gamma = 90^\circ$
Volume	$3549(2) \text{ \AA}^3$
Z	8
Density (calculated)	$1.559 \text{ mg/m}^3$
Absorption coefficient	$0.345 \text{ mm}^{-1}$
F(000)	1696
Crystal size	$0.488 \times 0.469 \times 0.281 \text{ mm}^3$
Theta range for data collection	2.167 to $27.454^\circ$
Index ranges	$-23 \leq h \leq 24$ , $-8 \leq k \leq 8$ , $-37 \leq l \leq 37$
Reflections collected	12785
Independent reflections	7214 [R(int) = 0.0332]
Completeness to theta = $26.000^\circ$	99.3 %
Absorption correction	Semi-empirical from equivalents
Max. and min. transmission	1.0000 and 0.76099
Refinement method	Full-matrix least-squares on $F^2$
Data / restraints / parameters	7214 / 117 / 562
Goodness-of-fit on $F^2$	1.106
Final R indices [ $I > 2\sigma(I)$ ]	R1 = 0.0488, wR2 = 0.0999
R indices (all data)	R1 = 0.0526, wR2 = 0.1027
Extinction coefficient	n/a
Largest diff. peak and hole	0.252 and $-0.261 \text{ e.}\text{\AA}^{-3}$

10.  $^1\text{H}$  NMR and  $^{13}\text{C}$  NMR spectra.

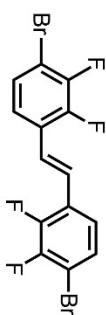


23F1bv

150.62  
150.44  
150.29  
150.10  
147.23  
146.99  
146.80

127.84  
127.79  
126.06  
125.93  
123.11  
123.04  
122.07  
122.03  
121.98

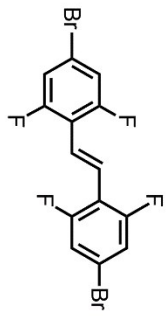
109.77  
109.52



9.0 8.5 8.0 7.5 7.0 6.5 6.0 5.5 5.0 4.5 4.0 3.5 3.0 2.5 2.0 1.5 1.0 0.5 0.0 -0.5

2.00  
4.00

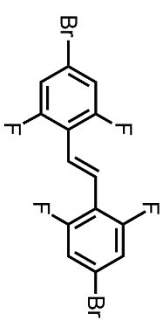
7.330  
7.157  
7.148  
7.136  
7.108  
7.096  
7.087

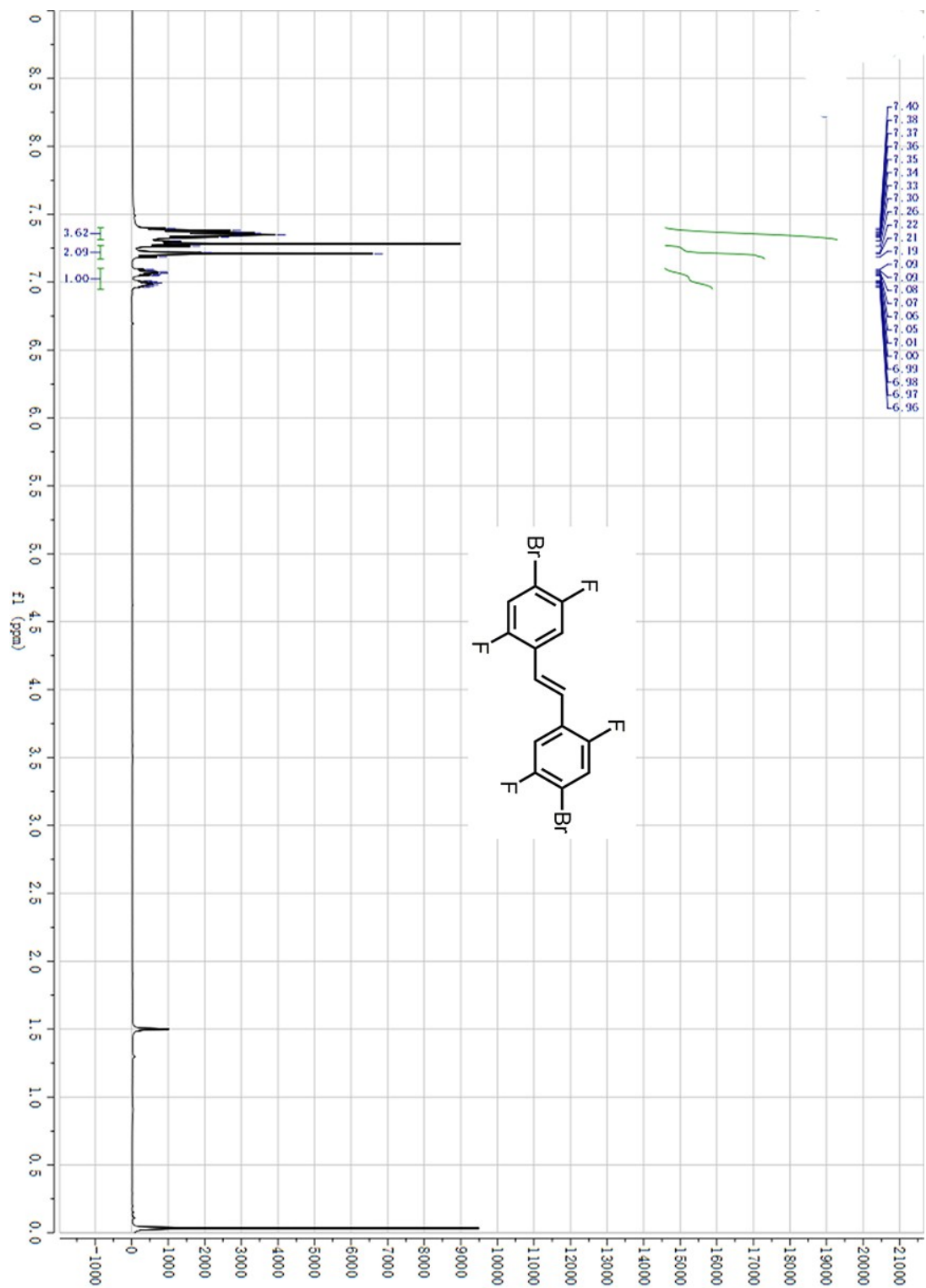


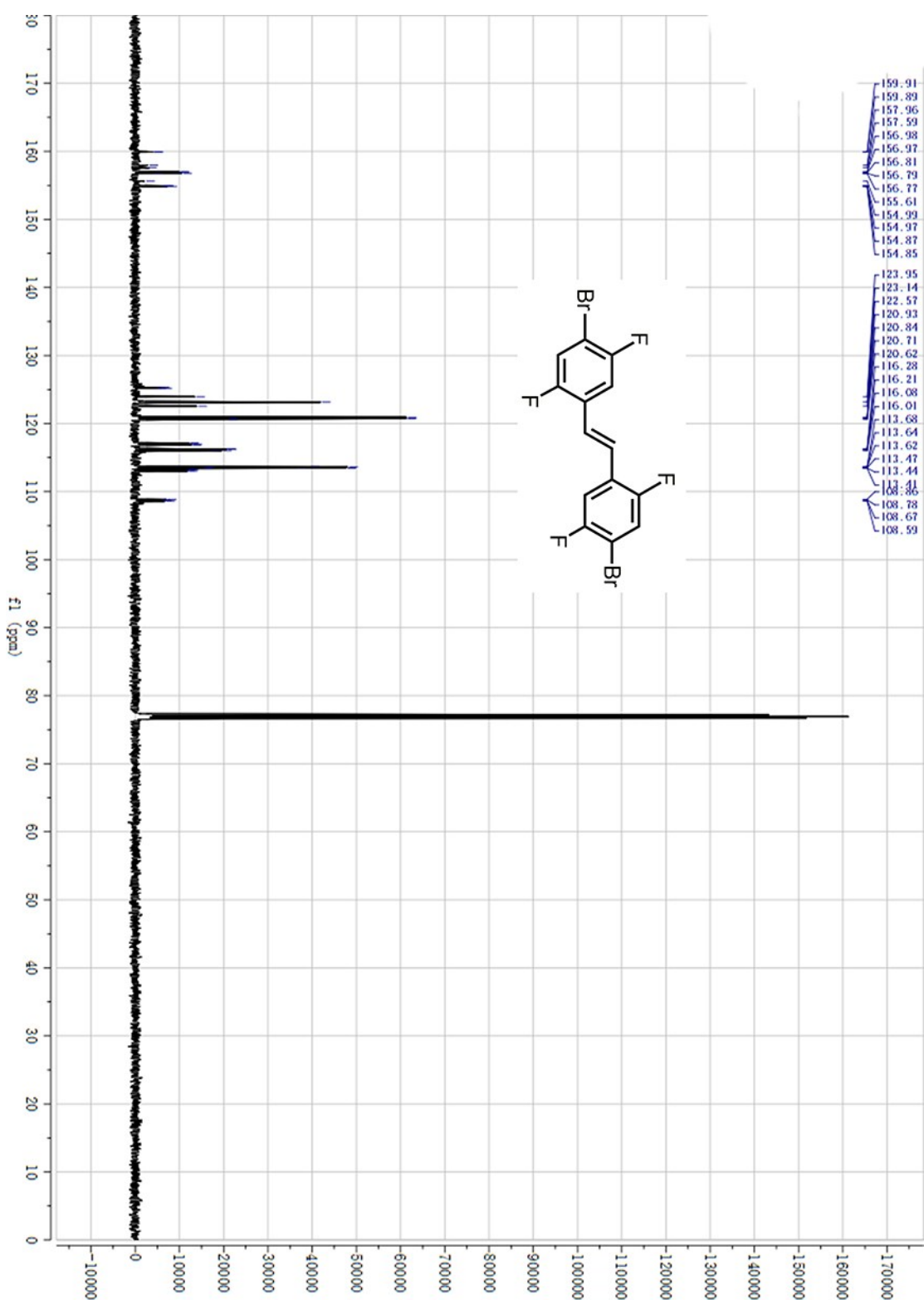
26-tfbv

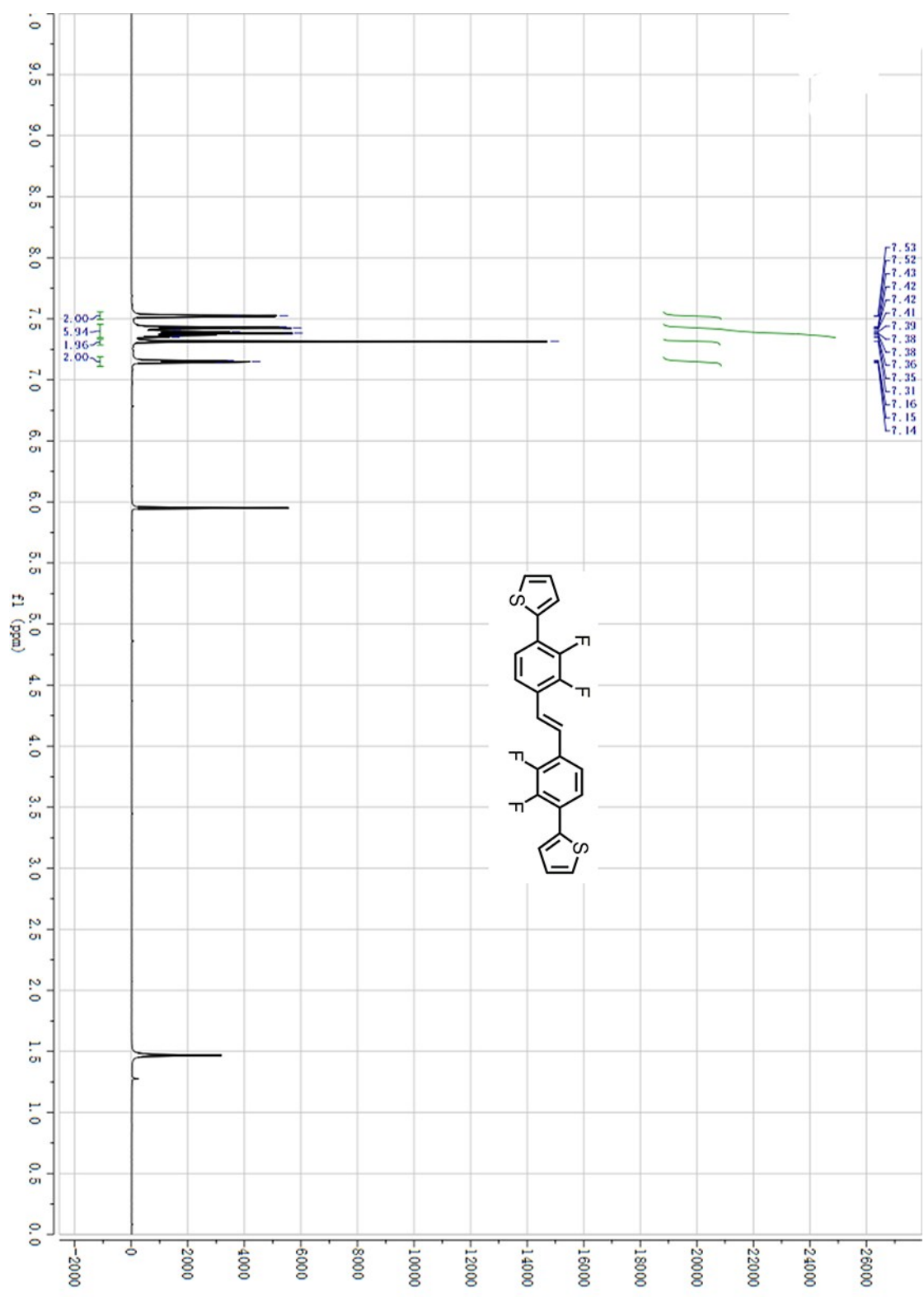
162.42  
162.31  
159.02  
158.91

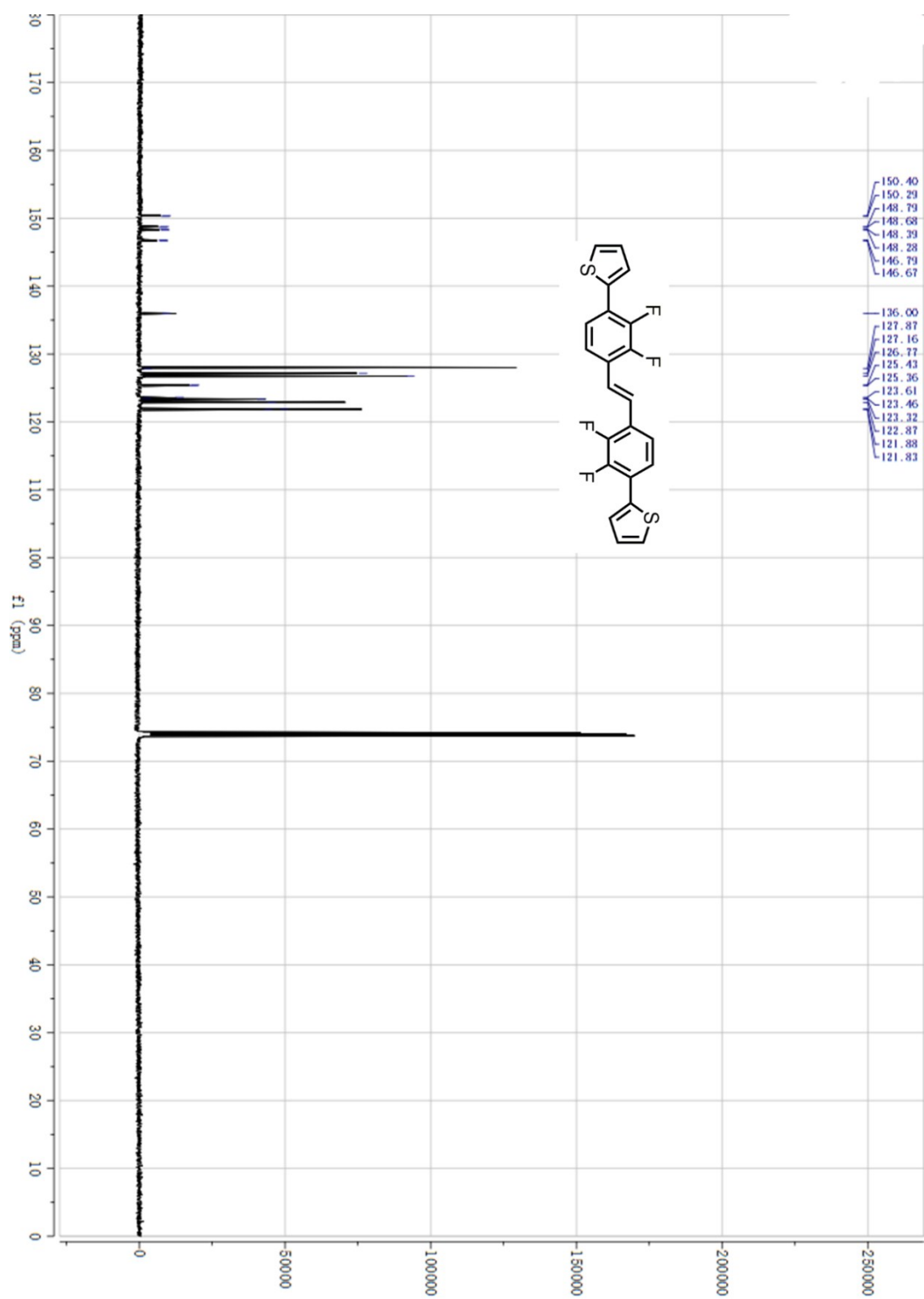
121.63  
121.51  
121.39  
121.01  
120.84  
120.67  
115.95  
115.92  
115.82  
115.68  
115.58  
115.55  
114.24  
114.04  
112.84

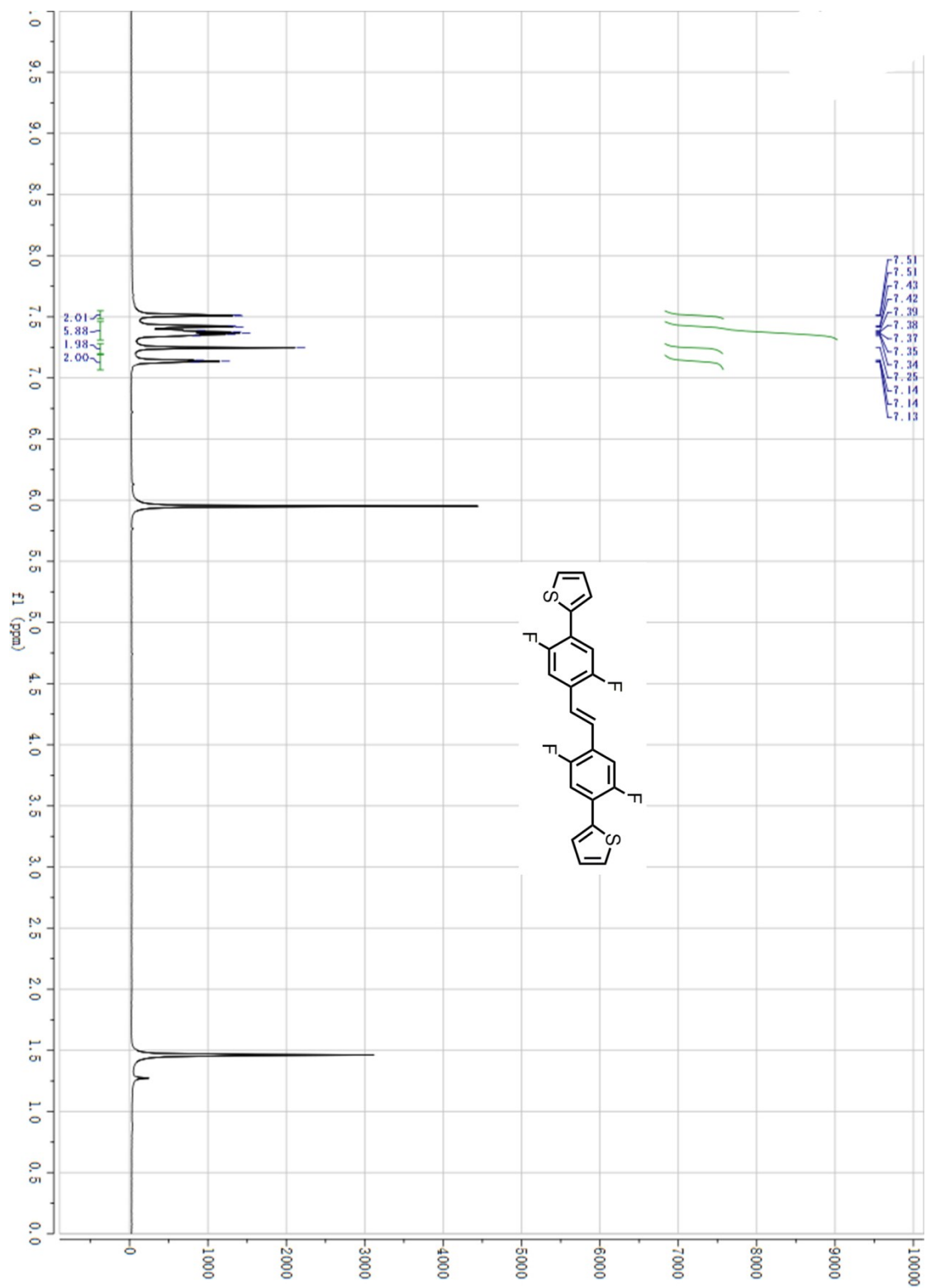


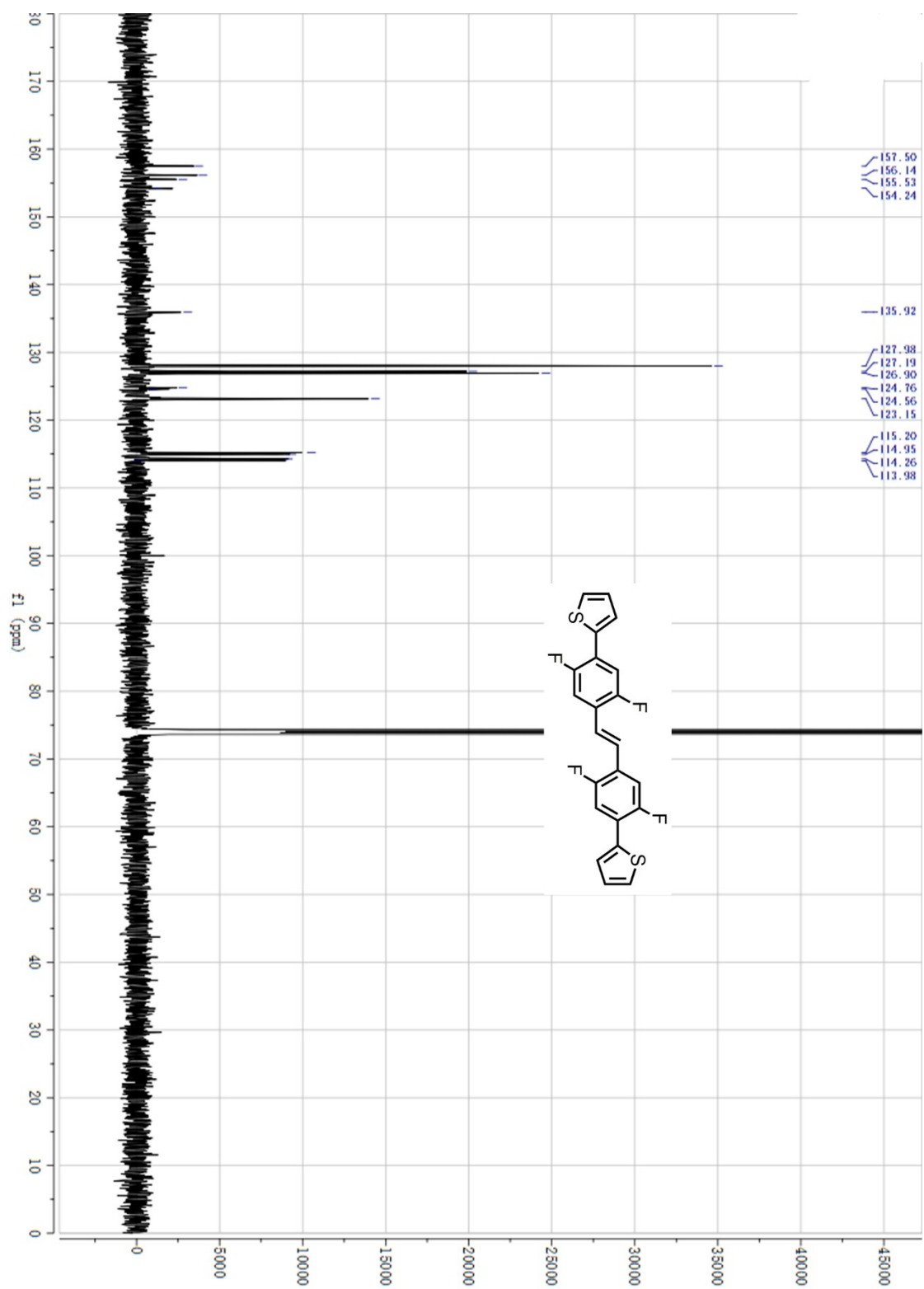












# PD23TFPE

